Geoderma 442 (2024) 116805

Contents lists available at ScienceDirect

Geoderma

journal homepage: www.elsevier.com/locate/geoderma

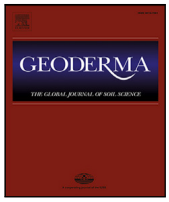

Spatial evaluation of the soils capacity and condition to store carbon across Australia

Alexandre M.J.-C. Wadoux [*,1], Mercedes Román Dobarco[2], Wartini Ng, Alex B. McBratney

Sydney Institute of Agriculture & School of Life and Environmental Sciences, The University of Sydney, New South Wales, Australia

ARTICLE INFO

Handling Editor: Jan Willem Van Groenigen

Keywords:
Soil security
Organic carbon
Potential
Soil properties and functions
Indicator
Soil multifunctionality

ABSTRACT

The soil security concept has been put forward to maintain and improve soil resources *inter alia* to provide food, clean water, climate change mitigation and adaptation, and to protect ecosystems. A provisional framework suggested indicators for the soil security dimensions, and a methodology to achieve a quantification. In this study, we illustrate the framework for the function soil carbon storage and the two dimensions of soil capacity and soil condition. The methodology consists of (i) the selection and quantification of a small set of soil indicators for capacity and condition, (ii) the transformation of indicator values to unitless utility values via expert-generated utility graphs, and (iii) a two-level aggregation of the utility values by soil profile and by dimension. For capacity, we used a set of three indicators: total organic and inorganic carbon content and mineral associated organic carbon in the fine fraction (MAOC) estimated via their reference value using existing maps of pedogenons and current landuse to identify areas of remnant genosoils (total organic and inorganic carbon) and the 90th percentile for MAOC. For condition we used the same set of indicators, but this time using the estimated current value and comparing with their reference-state values (calculated for capacity). The methodology was applied to the whole of Australia at a spatial resolution of 90 m × 90 m. The results show that the unitless indicator values supporting the function varied greatly in Australia. Aggregation of the indicators into the two dimensions of capacity and condition revealed that most of Australia has a relatively low capacity to support the function, but that most soils are in a generally good condition relative to that capacity, with some exceptions in agricultural areas, although more sampling of the remnant genosoils is required for corroboration and improvement. The maps of capacity and condition may serve as a basis to estimate a spatially-explicit local index of Australia's soil resilience to the threat of decarbonization.

1. Introduction

The valuation of functions provided by soils has aroused considerable attention recently (Baveye et al., 2016; Greiner et al., 2017). In the political decision-making arena, reference to the soil functions has led to several proposals for a soil policy promoting a sustainable use of soils. In Europe, for example, the European Commission scheduled a Soil Framework Directive (European Commission, 2006a) building on the Thematic Strategy for Soil Protection (European Commission, 2006b) in which soils are recognized for the set of functions they provide. Many countries and international organizations (e.g. the Food and Agriculture Organization, see FAO and ITPS, 2015) have subsequently built on the concept of multifunctional soils as a driver for policy and as a means to go beyond the valuation of soil in terms of their sole economic value. Soils do support agricultural production but are at the same time essential for providing a set of services that benefit both land owners as well as human societies (Breure et al., 2012). Most end-users, indeed, perceive soils through how they provide us food, fibre, biomass and raw materials, how they store and clean the water, sequester carbon to mitigate climate change and host nutrients and biodiversity.

The quantification of soil functions is, however, a scientific challenge (Vogel et al., 2019; Wadoux et al., 2021; Zwetsloot et al., 2021). Part of the difficulty lies in obtaining a direct measurement of soil functions (Baveye et al., 2016). Despite examples where a function is relatively easy to estimate through measurement of a single indicator (e.g. primary productivity estimated with the net total harvest, Vrebos et al., 2021), functions usually cannot be measured and must instead be estimated indirectly with a set of measurable soil properties that are used as indicators for the delivery of a specific function.

* Correspondence to: Laboratory of soil-agrosystem-hydrosystem interaction (LISAH), 2 place Pierre Viala, 34090 Montpellier, France.
E-mail address: alexandre.wadoux@inrae.fr (A.M.J.-C. Wadoux).
[1] Current affiliation: LISAH, Univ. Montpellier, AgroParisTech, INRAE, IRD, Institut Agro, Montpellier, France.
[2] Current affiliation: BC3 - Basque Centre for Climate Change, Scientific Campus of the University of the Basque Country, Leioa, Spain.

https://doi.org/10.1016/j.geoderma.2024.116805
Received 26 May 2023; Received in revised form 25 October 2023; Accepted 30 January 2024
Available online 3 February 2024
0016-7061/© 2024 The Author(s). Published by Elsevier B.V. This is an open access article under the CC BY-NC-ND license (http://creativecommons.org/licenses/by-nc-nd/4.0/).

Several modelling approaches have been developed in the literature to solve this difficulty (Greiner et al., 2017; Bünemann et al., 2018), and rely either on detailed process-based understanding using biophysical models or mechanistic relationships (e.g. Vogel et al., 2018) or on rule-based empirical techniques that combine several soil indicators (e.g. Van Leeuwen et al., 2019). Biophysical estimation is the most common approach as it does more justice to the soil chemical, physical and biological processes and is suited to model soil change over time and response of a soil to external perturbations (Choquet et al., 2021), though it can be very data demanding and time consuming. Approaches based on empirical rules were introduced in Andrews et al. (2004) in which an overall index of soil quality was obtained through aggregation of several indicators transformed into continuous dimensionless scores. There are of course earlier attempts via the calculus of land evaluation (e.g. Rossiter, 1996), but this approach has made its way into soil science under the umbrella of soil quality (Seybold et al., 2018; Bünemann et al., 2018), soil health (Lehmann et al., 2020), soil-based ecosystem services (Calzolari et al., 2016) and more recently soil security (McBratney et al., 2014; Evangelista et al., 2023a) assessment. Hereafter, we follow the approach based on the combination of dimensionless indicators representing utility to support a soil function.

What is evident is that soils can be altered as a result of human intervention, pressure of agriculture and degradation processes (e.g. loss of topsoil due to accelerated erosion). For the quantification of soil functions, Vogel et al. (2019) proposed a concept to separate the soil potential to fulfil a function and its actual state for doing so. The intrinsic potential refers to the maximum ability of a soil under optimum soil management strategies for performing a soil function. The quantification of a soil function delivery potential is made with inherent soil indicators that are slowly changing and not readily altered by human intervention. The actual state, conversely, includes in the assessment dynamic properties and properties affected by soil management, some of which may be rapidly changing (e.g. pH, microfauna and microflora). Accounting for both potential and current state of functions has been briefly considered in the assessment of soil quality (see Seybold et al., 2018, Section VI-B), although it did not seem to find support in later studies. In the soil security concept (McBratney et al., 2014), both potential of a soil and current state are explicitly accounted for through the two biophysical dimensions of capacity and condition, but they are not equivalent. While the concepts are relatively new and still evolving, the capability of a soil to perform a function will be limited by its capacity (determined by inherent soil properties) and affected by its condition (current state) which responds to management and land use history (Evangelista et al., 2023b). The difference between potential and capacity is that while both are determined by soil inherent properties and site conditions, the potential (*sensu* Vogel et al., 2019) corresponds to a soil which condition is modified in the direction that better suits the management objective given its capacity. The capacity will limit the performance of that function irrespective of the best management practices. Assessing soil capacity therefore raises the question of how to define a reference state of soil.

The quantification of capacity and condition was in consequence linked with the pedogenon–pedophenon concept in Román Dobarco et al. (2021a) and Evangelista et al. (2023a). This is different from Vogel et al. (2019) in which potential and current state were quantified using sets of indicators representing stable and dynamic properties, respectively. A genoform or genosoil is a genetic soil type or a soil system under quasi steady-state. It was defined by Rossiter and Bouma (2018) as "soil classes as identified by the soil classification system used as basis for detailed soil mapping in a given area". A recent definition of genosoils refers to soils that result from the legacies of natural and anthropedogenesis, but that have been least affected by contemporary drivers of soil change since a reference time (Román Dobarco et al., 2023a). The phenoform or phenosoil is a permanent variant of a genoform resulting from change in soil management and land use with sufficient differences to affect soil functions. Genosoils and phenosoils are a convenient way to quantify the capacity and condition of a soil to fulfil a set of functions. This can be made using a relative approach: The genosoil represents the inherent capacity of the soil to provide a function with minimum (contemporary) management, it is a baseline or reference. The ability of a phenosoil to provide functions (i.e. capacity + condition) is quantified with respect to the ability of its genosoil (i.e. the capacity). The phenosoil may have greater condition than the genosoil, and hence become the management target.

The objective of this study was to make this concept operational and provide a first large-scale evaluation of a soil function following the soil security framework (Evangelista et al., 2023b). The aim of this paper is also to illustrate a component of the recently-proposed soil security assessment framework. We demonstrate the concept using the function soil carbon storage. We describe the methodology and the approach to quantify the capacity and condition using a set of indicators and an existing map which we use to derive reference soils. The methodology is tested for the whole of Australia. The proposed methodology is then discussed and ways to improve the concept are presented.

2. Materials and methods

2.1. Capacity and condition of soils to store carbon

The spatial evaluation and quantification of capacity and condition of Australian' soils to store carbon consists of three steps. First, the function is characterized by a small set of soil indicators in accordance with usual approaches in soil quality and soil health assessment (Seybold et al., 2018; Rinot et al., 2019). Second, the indicators are transformed to unitless utility scores with utility graphs (also known as scoring functions, e.g. see Andrews et al., 2004). The utility graph converts the values of the soil indicator to a range between 0 and 1, depending on how the value of the indicator supports the function. Third, the various scores are combined at two levels, by soil profile and by dimension, to provide a single spatially-explicit index of soil capacity and condition. We describe these three steps in the following three paragraphs.

Selection and quantification of soil indicators for capacity and condition. Various studies have described the practical and conceptual requirements for selecting a set of soil indicators to evaluate functions provided by soils (e.g. Arshad and Coen, 1992; Doran and Parkin, 1994; Nortcliff, 2002; Bünemann et al., 2018). We consider an approach consisting of selecting a minimum dataset of soil indicators that are relevant to the function soil as a store of carbon. In this case, the minimum dataset selection is inferred from expert judgement and the selected properties have known influential relationship with the function. The indicator dataset to assessing the condition of the function consists of total organic carbon (TOC), inorganic carbon (TIC) and mineral associated organic carbon (MAOC). For the capacity we use the same set of indicators, but this time estimating their reference value. The reference values of TOC and TIC are obtained using information from auxiliary variables to obtain the location of remnant genosoils. This is done by comparison of a pedogenon map and information on current landuse. The capacity of the soil for storing MAOC in the fine fraction ($\leq$50 μm) is estimated applying the C saturation concept (Six et al., 2002). Hereafter, the indicators for capacity are the genosoil TOC and TIC (Sharififar et al., 2023), and the upper limit of a model of the C saturation (Table 1).

Transformation of indicators to unitless scores. The selected soil indicators for capacity and condition have different units and range of values. To combine indicators with different units we use a standard technique in soil quality and health assessments based on scoring functions. The utility graph converts the values of the indicator to a unitless score, called the utility. The utility is obtained from the shape of the utility graph that informs on relationship of the indicator and the performance of the function. We use standard shapes from the literature (Rinot et al., 2019) with optimum range and threshold

above which the function achieves its maximum according to the soils' capacity and condition. All utility graphs are continuous. For indicators where values are available at various soil depths, a single utility graph with depth-specific optimum range and threshold is constructed.

Aggregation of scores by profile and dimension. Multiple unitless scores are combined in two levels to come up with a quantification of a dimension for the function. First, the depth-specific scores of an indicator are combined for each soil profile. We suggest the average of the profile-specific value of the score. In the next level, the various unitless estimated of the indicators are aggregated through averaging to give a single value for the dimension (i.e. either capacity or condition) at each spatial location. We adopt an approach where maps of indicators are mapped before transformation with the utility graphs and aggregation. This approach is referred to as the "first interpolate then calculate" in the literature (e.g. Styc and Lagacherie, 2019).

Table 1
List of soil indicators for assessing the function soil as a store of carbon. The indicators differentiate the soil capacity and condition to fulfil the function.

Capacity	Condition
Genosoil TOC	Genosoil TOC - current TOC
Genosoil TIC	Genosoil inorganic TIC - current TIC
90th MAOC	Current MAOC/90th percentile MAOC

2.2. Study area and data

2.2.1. Study area - Australia

The study area includes continental Australia and Tasmania, which span six climatic zones according to the Köppen classification: equatorial, tropical, subtropical, desert, grassland and temperate (Bureau of Meteorology, 2023). The relief in the continent is generally flat, and areas of higher elevation are found in several highlands and the Great Dividing Range, towards the east. The major agricultural areas are located in the eastern areas of Queensland and New South Wales, Victoria, south of South Australia and the south-western area of Western Australia, along the Australian wheatbelt (ABARES, 2021). While cropping occupies less than 5% of the area, grazing in native vegetation (42%) or modified pastures (6%) increase the extent of primary production to rangelands (ABARES, 2021). On the other hand, nature conservation or protected managed resources cover 28% of Australia (ABARES, 2021).

2.2.2. Soil data

TOC. We use a set of 90,025 preprocessed organic carbon concentration (in %) measurements from the study of Wadoux et al. (2023), preprocessing of which we briefly summarize here. The TOC data were collected from various Australian institutions via the SoilDataFederator, an open web API managed by CSIRO (Searle et al., 2021). We selected TOC data for the period 1970–2020 to obtain a sufficiently large dataset. The different units present in the data collection from the web API were harmonized, while duplicated measurements and wrong entries were removed. We set upper limits for the TOC concentration according to the published literature and accounting for biome and landuse. This was done to exclude unrealistic TOC values. We then built continuous depth function of TOC using a mass preserving equal area quadratic spline (Bishop et al., 1999; Malone et al., 2009). This resulted in six continuous depth intervals over the soil profile, from which we extracted TOC data from the 0–5 cm, 5–15 cm, 15–30 cm, 30–60 cm, 60–100 cm, and 100–200 cm depth intervals. Boxplots of the TOC data used in this study after data cleaning and depth standardization are categorized by biome in Wadoux et al. (2023, Fig. 1).

TIC. The soil total inorganic carbon content data were compiled from two datasets: SoilDataFederator, the web API managed by CSIRO (Searle et al., 2021) and from the National Geochemical Survey of Australia (NGSA). Samples from the web API span 4465 unique sites across various depths, but only measurements for the depth interval 0–200 cm are kept. Inorganic carbon collected in the web API were measured using various methods: rapid titration, pressure change (manometric and transducer), but all reported as % calcium carbonate. Samples from the NGSA were collected across 1311 unique sites across Australia. Measurements of TIC are available for two depth intervals: 0–10 cm and 60–80 cm. The NGSA soil sample collection and preparation is described in details in Lech et al. (2007) and De Caritat and Cooper (2011) respectively, while the compilation of digestion and analytical methods were described in de Caritat et al. (2009). The calcium carbonate concentration (%) from the NGSA dataset was calculated based on the total calcium oxide concentration determined by X-ray Fluorescence analysis reported in the NGSA geochemical database using the Linear programming code "LPNORM" (de Caritat et al., 1994). Observations across different depths are then standardized following the 0–5 cm, 5–15 cm, 15–30 cm, 30–60 cm, 60–100 cm, and 100–200 cm depth intervals using a mass preserving equal area quadratic spline (Bishop et al., 1999; Malone et al., 2009), the same way as for the TOC.

MAOC. In this study we reuse a dataset of spectral predictions on MAOC content derived from the SOC fractionation dataset by Baldock et al. (2013a). MAOC was estimated as the organic carbon found in the fine fraction (≤50 μm) excluding the content of poly-aril C (biochemically recalcitrant carbon) measured with soil-state ^{13}C nuclear magnetic resonance spectroscopy (Baldock et al., 2013a). MAOC concentration (mg MAOC-C g^{-1} soil) was predicted with three spectral calibration models (Baldock et al., 2013b; Malone, 2020; Malone and Wadoux, 2022) on georeferenced topsoil samples (between 0–30 cm depth) from the Australian Soil Carbon Research Program (SCaRP) (Baldock et al., 2013b), the Australian Soil Archive mid-infrared spectral library (Hicks et al., 2015), and the expanded Australian Soil Archive visible and near-infrared spectral library (Viscarra Rossel and Hicks, 2015; Malone et al., 2020). More detailed information on the spectral datasets, processing and predictions can be found in Román Dobarco et al. (2023b). The MAOC predictions were processed to eliminate duplicates and unrealistic extreme values (e.g., MAOC ≥ 100 mg C g^{-1} soil). MAOC concentrations were standardized for the 0–30 cm with equal-area quadratic splines (Bishop et al., 1999). This resulted in a total of 14,592 predictions of MAOC concentration for 0–30 cm across Australia, mostly from croplands and pastures (Fig. 1).

2.2.3. Soil maps

TOC. A large set of spatially-exhaustive environmental covariates covering Australia were collected and processed to conform with a spatial resolution of 90 m × 90 m and to the same spatial extent. The covariates represent factors influencing TOC spatial variation such as climate, topography, parent material, organisms/vegetation and other soil properties. The preprocessed measured TOC data of Section 2.2.2 and their corresponding value of environmental covariates were used to fit a random forest machine learning model (Breiman, 2001) for each depth interval. The fitted depth-specific models were validated using 10-fold cross-validation. Prediction was then made with a quantile regression forest model fitted on all the data. The maps of TOC along with uncertainty intervals are freely available in Wadoux et al. (2022). The full list of covariates along with more information on the preprocessing procedure, model fitting, validation and prediction are provided in Wadoux et al. (2023).

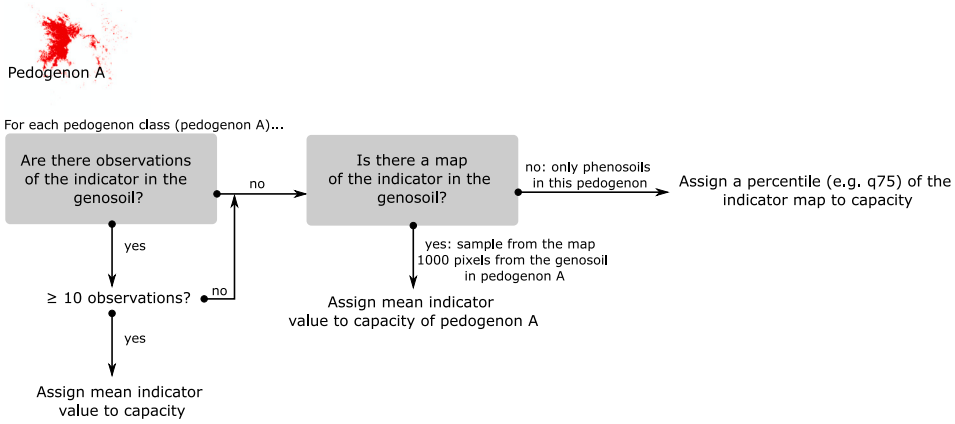

Fig. 1. Summary workflow of the steps required to assign an average value of the indicators (i.e. TOC and TIC) for each pedogenon class using the current landuse to obtain areas of remnant genosoils, measured values of the indicators and maps of the indicator.

TIC. Mapping of TIC was done with the same environmental covariates as for TOC. A two-step procedure was used to account for the zero-inflated and skewed measurements of carbonates in soil. First, a classification random forest model was fitted to predict the presence/absence of carbonates. In a second step, a quantile regression random forest model was fitted on all non-zero values. The final prediction of TIC is taken as the product of the prediction from the two steps. Model fitting and validation follow the procedure for mapping of TOC previously described.

MAOC. Maps of the MAOC content across Australia were predicted with a generalized additive model (GAM) using the mgcv package (Wood, 2022) in R. Prior to model construction, a cubist model was fitted to MAOC concentration as response variable and a set of 45 soil and environmental covariates (climate and parent material) as predictor variables. The soil variables consisted of silt + clay content calculated from the Soil and Landscape Grid of Australia (Malone and Searle, 2021) and soil pH. The climate and parent material variables were all available in the TERN Digital Soil Mapping Raster Covariates Stacks v2 (Searle et al., 2022). The rules of the cubist model were used to define geographical regions with similar environmental control of MAOC levels. The cubist rule was included as a categorical variable in the GAM models. A subset of candidate variables was first selected from exploratory data analysis. Univariate GAM models were fitted for each candidate variable and compared with the null model using the Akaike information criterion (AIC). A full model was then fitted with the best four soil, four parent material, and six climate variables. The final model was selected with manual backward selection based on 10-fold cross-validation statistics (average AIC, mean error, root mean squared error (RMSE), coefficient of determination (R^2) and concordance correlation coefficient). When the GAM model requirements were not met (normality of residuals, lack of concurvity) for the model with the best cross-validation statistics, we compared the sub-optimal model with "leave one variable out" models and eliminated problematic variables successively until the optimal model was found.

2.2.4. Auxiliary variables

Pedogenon map. Pedogenon classes are conceptual taxa that define groups of homogeneous environmental variables (Román Dobarco et al., 2021b). These groups are created applying unsupervised classification (e.g. *k*-means clustering) to a set of state variables, proxies of the soil-forming factors for a given reference time. The assumption is that the soil-forming processes within these classes (i.e. pedogenons) have been relatively similar over pedogenetic time and thus have developed soils with similar properties. We used the pedogenon map for Australia (Román Dobarco et al., 2022, 2023a) that consists of 1370 pedogenon classes. The reference time for defining soil entities at quasi steady-state is the European settlement in Australia, in the second half of the XVIII century.

Land use map. The Catchment Scale Land Use of Australia dataset (CLUM) at 50 m × 50 m resolution (ABARES, 2021) has 18 land use classes that were reclassified into two categories to differentiate soils in a natural or relatively natural areas from soils with intensive use. Categories falling into natural and relatively natural areas were land uses categorized as conservation areas, or as production from relatively natural environments: nature conservation, managed resource protection, other minimal use, grazing native vegetation and production native forest. All other classes were assigned to intensive use (dryland and irrigation cropping, grazing in modified pastures, and forestry) while urban areas and water bodies were disregarded.

The pedogenon map and the binary land use map (natural/intensive) were overlayed to define genosoils and phenosoils subclasses for each pedogenon class. Natural or relatively natural areas corresponded to genosoils, whereas intensive uses (cropping, grazing, forestry) were aggregated into phenosoil category.

2.3. Capacity

For any location **s** in the study area, the capacity of a soil to store carbon is calculated as a function of the TOC and TIC of the genosoil denoted TOC_{gen} and TIC_{gen} (in %), respectively, and by the upper limit of the organic carbon concentration in the MAOC ($MAOC_{upper}$, in %) fraction (≤ 50 μm):

$$C_{cap} = f\left(u(TOC_{gen}), u(TIC_{gen}), u(MAOC_{upper})\right), \quad (1)$$

where C_{cap} is a unitless value of the degree of fulfilment of the soil's capacity to store carbon. The function f relates the unitless value of the indicators at location $\mathbf{s}_i$ to C_{cap}, and u is a continuous function (hereafter denoted utility graph) that return a unitless value between zero and unity of the indicator.

The TOC and TIC contents of the genosoils are estimated for each pedogenon class (Román Dobarco et al., 2021b) using measured values and predicted maps of TOC and TIC. The approach relies on the identification of remnant genosoils with information on current landuse. Areas within a pedogenon class that are under a current natural and relatively natural land use are considered as genosoils from which we can obtain information on the TOC and TIC content. We refer to the workflow in Fig. 1 for the various steps required to obtain an average value of the indicator for each pedogenon class.

The soil profile at location $\mathbf{s}_i$ is composed of several depth intervals from which soil observations or maps are available. Both $u(TOC_{gen})$ and $u(TIC_{gen})$ are estimated through averaging of the depth-specific utility graphs:

$$u(TOC_{gen}) = \frac{1}{D}\sum_{d=1}^{D} u(TOC_{gen})_d, \quad (2)$$

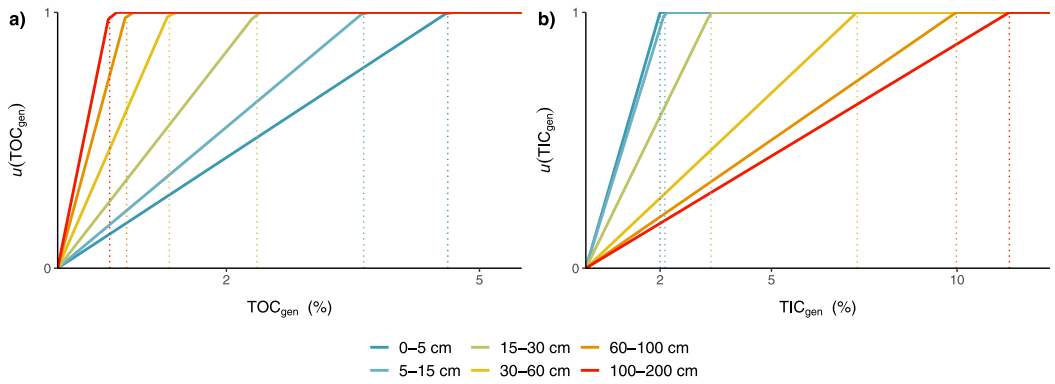

Fig. 2. Utility graphs of the depth-specific functions $u(\mathrm{TOC}_{\mathrm{gen}})$ and $u(\mathrm{TIC}_{\mathrm{gen}})$, for all depth intervals. The utility graphs $u(\mathrm{TOC}_{\mathrm{gen}})$ and $u(\mathrm{TIC}_{\mathrm{gen}})$ and aggregated into a single graph for the whole profile by averaging.

$$u(\mathrm{TIC}_{\mathrm{gen}}) = \frac{1}{D}\sum_{d=1}^{D} u(\mathrm{TIC}_{\mathrm{gen}})_d, \tag{3}$$

where d is the depth interval considered and D is the total number of depths intervals. Utility graphs for Eqs. (2) and (3) are illustrated in Fig. 2. Threshold values determining optimal capacity with respect to the indicator value is different for each depth interval. We assumed a threshold corresponding to the 90th percentile of the depth-specific TOC and TIC observations, respectively.

The carbon concentration of the MAOC fraction was estimated following the C saturation approach (Six et al., 2002). The C saturation refers to a limited capacity of the mineral matrix to protect SOC against microbial decomposition through physico-chemical stabilization mechanisms, e.g., physically isolated inside microaggregates, or chemically bonded to surfaces of mineral particles. SOC is also protected by its inherent biochemical recalcitrance, whereas the particulate organic carbon pool is less protected against decomposition (Six et al., 2002; von Lützow et al., 2006). The hypothesis of the C saturation concept suggests that the MAOC fraction reaches a maximum level after which it saturates (Cotrufo et al., 2019), and bulk SOC reaches a steady state irrespective of increasing C inputs (Stewart et al., 2007). While evidence of MAOC saturation is not found in every study region (Begill et al., 2023), e.g., in agricultural soils or areas where climate limits the organic matter input into the soil, the existence of a theoretical upper limit for MAOC stabilization controlled by soil mineralogy makes sense from the physical point of view and has been often estimated with boundary line analysis at different spatial scales (Feng et al., 2013; Georgiou et al., 2022). MAOC storage is controlled by inherent soil properties and geochemistry (e.g., clay and silt content, mineralogy, Fe and Al (hydr)oxides) (von Lützow et al., 2006; Doetterl et al., 2015), climate, vegetation, and land use. Therefore, the indicator for MAOC storage capacity was defined as the C saturation or upper limit of MAOC, which is a function of soil properties, parent material (as a proxy for soil geochemistry and mineralogy) and climate:

$$\mathrm{MAOC}_{\mathrm{upper}} = g(\mathrm{soil}, \mathrm{parent\ material}, \mathrm{climate}, \mathrm{vegetation}). \tag{4}$$

Mapping of $\mathrm{MAOC}_{\mathrm{upper}}$ at 90 m resolution was done applying quantile non-parametric additive models (qGAM) at every pixel. The C saturation model for Australia used the same soil and environmental variables as input, and the structure of the GAM model defined in Section 2.2.3. The qGAM model was fitted with the `qgam` package in R (Fasiolo et al., 2021). Land use and vegetation were excluded from the model for soil capacity since most observations originated from croplands and not all land cover types would be represented in the model. We assumed that whereas the upper limit of MAOC would be representative of pastures and closer to semi-natural systems, current MAOC content is a result of management and hence is more related to the condition dimension. Here too, the cubist rule was included as a categorical variable in the qGAM models. The upper limit of MAOC storage was predicted with a qGAM model that had the same model structure as for current MAOC content, but this time predicting the 0.90 percentile. The utility graph $u(\mathrm{MAOC}_{\mathrm{upper}})$ is shown in Fig. 3.

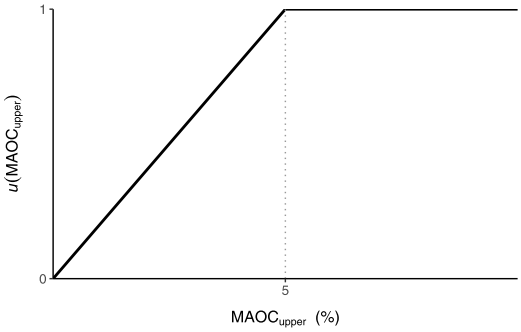

Fig. 3. Utility graph of the indicator $\mathrm{MAOC}_{\mathrm{upper}}$.

2.4. Condition

The current condition for TOC and TIC are calculated as the difference between the genosoil indicator value and the current value, that is, $u(\mathrm{TOC}_{\mathrm{gen}} - \mathrm{TOC}_{\mathrm{current}})$ and $u(\mathrm{TIC}_{\mathrm{gen}} - \mathrm{TIC}_{\mathrm{current}})$ for TOC and TIC, respectively. The utility graphs are shown in Fig. 4.

The content of MAOC is responsive to changes in land use and vegetation (Guo and Gifford, 2002; Dalal et al., 2021), although it is less responsive to management than the particulate organic carbon fraction (Rocci et al., 2021). The indicator for MAOC condition is calculated as the ratio between current MAOC and the upper limit of MAOC:

$$\mathrm{MAOC}_{\mathrm{cond}} = u\left(\frac{\mathrm{MAOC}_{\mathrm{mean}}}{\mathrm{MAOC}_{\mathrm{upper}}}\right). \tag{5}$$

The utility graph for the condition of MAOC is shown in Fig. 5.

Accordingly, the evaluation of the condition of the function $\mathrm{C}_{\mathrm{cond}}$ is calculated as follows:

$$\mathrm{C}_{\mathrm{cond}} = f\left(u(\mathrm{TOC}_{\mathrm{gen}} - \mathrm{TOC}_{\mathrm{current}}), u(\mathrm{TIC}_{\mathrm{gen}} - \mathrm{TIC}_{\mathrm{current}}), u(\mathrm{MAOC}_{\mathrm{mean}}/\mathrm{MAOC}_{\mathrm{upper}})\right). \tag{6}$$

3. Results

Fig. 6 shows the indicator maps after scoring the depth-specific values of the indicators and averaging by profile. The three maps have a different spatial pattern, although some general observations can be made. Most of Australia has low capacity (i.e. it has a value lower than

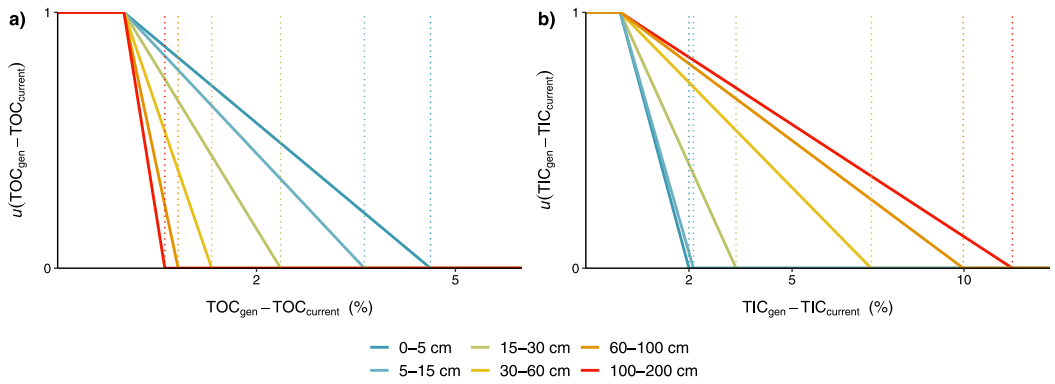

Fig. 4. Utility graphs of the depth-specific functions $u(TOC_{gen})$ and $u(TIC_{gen})$, for all depth intervals. The utility graphs $u(TOC_{gen} - TOC_{current})$ and $u(TIC_{gen} - TIC_{current})$ and aggregated into a single graph for the whole profile by averaging.

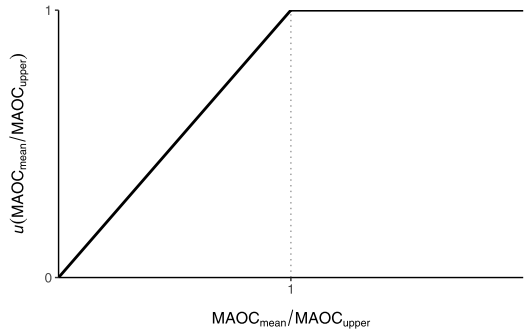

Fig. 5. Utility graph of the indicator $MAOC_{upper}$.

0.5) for the three indicators. A large arch, in particular, spanning from the Western coast of Perth, the large arid landscapes of central Australia, to the Eastern cost, has a very low capacity (i.e. lower than 0.3) for the three indicators. Tasmania and the Eastern coast of Australia have a relatively high capacity for the TOC indicator, as indicated by the values nearly always higher than 0.6. A different pattern is observed for TIC, where only the Calcarasol (Isbell and National Committee on Soil and Terrain, 2021) in the South coast of Australia have a very high value of the indicator. The MAOC shows that only Tasmania (peatland areas excluded) and Victoria have a high capacity for this indicator, and that large areas in the from the North-Eastern to the North-Western coast have a moderately high capacity.

The final C saturation model had as predictive variables clay+silt (%), pH, gamma radiometric thorium (ppm), gravity, annual precipitation, annual temperature range, and monthly maximum temperature (Fig. 7). The gam smooth terms indicated a positive model effect on MAOC concentration with increasing silt+clay content, a negative model effect of gravity, while the smooth parameter of thorium was highly variable across its range. Maximum temperature had a negative effect on MAOC concentration between 15–37 °C and then a positive model effect with 40 °C. The smoothing term for precipitation increased sharply between 0–1000 mm and then again between 2000–4000 mm. The smoothing term of temperature range and pH indicated a small effect of these variables on MAOC concentration. The parametric terms indicated smaller coefficients for the arid and temperate region of the wheatbelt. These effects explain the higher MAOC capacity towards the coast (with an increase in precipitation), the south (lower maximum temperature), and in areas with higher content of silt+clay. The final model had an AIC = 89 464 (compared to the worst model with AIC = 93 262). However, we obtained moderate results in 10-fold cross-validation, with an $R^2 = 0.25$ and a RMSE of 8.5 mg MAOC-C g^{-1} soil.

Fig. 8 shows the maps of indicators for condition after scoring the depth-specific values and averaging by profile. There is a clear difference in the overall appearance of the maps of condition for TOC and TIC in contrast with that of MAOC: the maps of TOC and TIC show high (i.e. higher than 0.9) value of condition for most Australia whereas the map of MAOC is more contrasted with an overall a moderate value (i.e. around 0.6). There is, however, an important spatial variation in the indicator value. The TOC map shows that the condition is low in many agricultural areas in the Eastern coast of Australia, in Northern Tasmania, and in small areas in the North and in the South-Western coast. A slightly similar pattern is observed for TIC with the exception of the South-Eastern cost (i.e. low values for TOC but high values for TIC), with in addition very low values of condition observed in a large band South of Australia, and in small areas in the Western and North-Eastern coast. The pattern is more complex to interpret for MAOC: there is large variation in the indicator value around a value of 0.5–0.7 but a large area in the South of Australia has a low condition value (i.e. lower than 0.2) for this indicator. Areas with moderate-high condition occur in areas with relatively low capacity that are not dedicated to agriculture and are hence closer to saturation.

Fig. 9 shows the maps of capacity and condition obtained after averaging of the indicators of capacity (Fig. 6) and condition (Fig. 8), respectively. The map of capacity shows that most of Australia has generally low capacity. This was also visible in the indicator maps of Fig. 6. A large band spanning the Southern coast including Tasmania and the Eastern coast of Australia have a higher capacity than the rest of Australia, with values higher than 0.5. This reflects the influence of TIC on southern Australia and overall higher TOC and MAOC following the climate gradient. The map of condition has a detailed spatial pattern with large variation. Most of Australia has a relatively good condition for the function, with some exceptions in a small band near the western coast and in small patches in the south of Australia.

4. Discussion

The spatial pattern of capacity and condition seemed realistic and generally agreed with existing knowledge of soil storage capacity and soil carbon loss in Australia and with national (e.g. Wadoux et al., 2023; Román Dobarco et al., 2023b) and regional (e.g. Wang et al., 2018; Gray et al., 2019) maps of soil organic carbon concentration, stocks and fractions, although some anomalies are observed. As a test, we further calculated the condition for the tospoil TOC only. Fig. 10 was derived to find areas where the topsoil TOC is potentially deteriorated due to agriculture. The map was obtained after scoring and averaging by profile for the depth intervals 0–5 cm, 5–15 cm and 15–30 cm. Areas potentially deteriorated exist where the condition is lower than 0.9. We found, conversely, that this map reflected better existing knowledge of SOC loss due to Agriculture in Australia. The anomalies observed

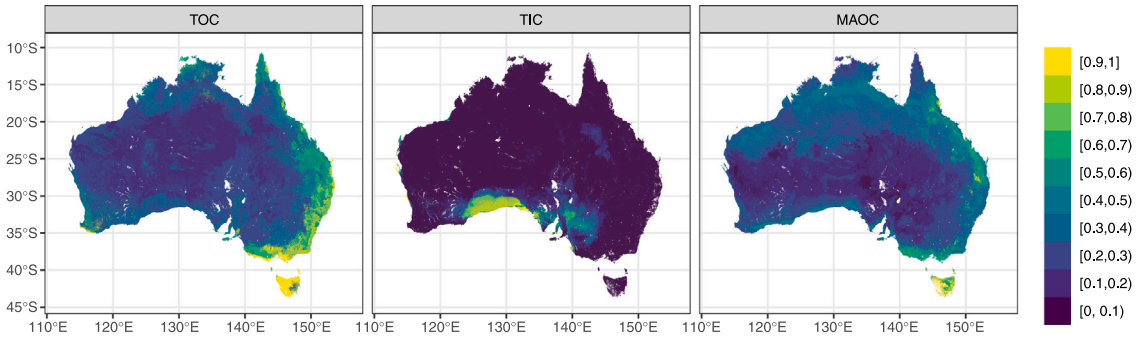

Fig. 6. Maps of the three indicators of capacity obtained after averaging by profile.

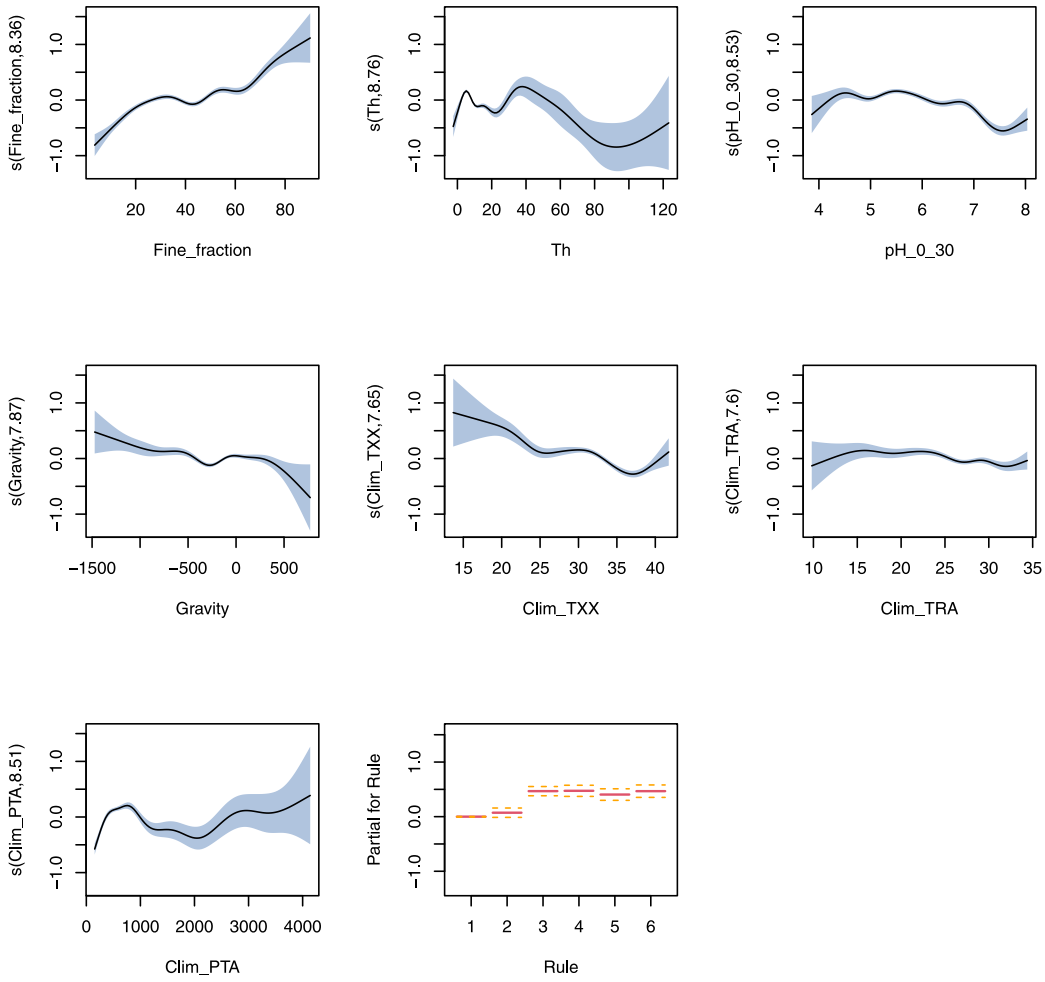

Fig. 7. Smoothing parameters of the GAM model for current MAOC content.

in the map of condition of Fig. 9b occurred mostly in agricultural areas where agricultural practices are known to affect soil organic carbon but this was not clearly reflected in the map of condition. In the Hunter valley (North-Eastern New South Wales), for example, a soil with similar capacity (i.e. same soil type and climate) might show various conditions depending on use (e.g. cropping versus grazing on native pasture, Wells et al., 2019). Sanderman et al. (2017) estimated the soil organic carbon loss in Australia to be 10 Pg C, standing out as a hotspot country of SOC loss. In New South Wales, Gray and Bishop (2016) estimated the average change in organic carbon resulting from 12 scenario predictions, and showed a loss of 193 Tg of organic carbon is to be lost by 2070 with the current rate of change. These estimates from the literature, however, did not translate well into lower scores of TOC condition. The anomalies might be caused by the lack of data within the genosoils, which makes accounting for differences in land uses a challenging task (see also Fig. 1). The genosoils, mainly comprising remnant vegetation, tend to be relatively undersampled compared with the phenosoils, so targeted sampling of the genosoils would help to improve the estimation of both capacity and especially condition. Another cause of the anomalies might be that land use was ignored when calculating the condition maps, although it was indirectly taken into account through the calculation of the difference with the indicators for capacity.

Similarly, land use was not included in the GAM model since most MAOC observations originated from croplands and pastures. Obtaining MAOC observations from semi-natural areas (forests, woodlands, native

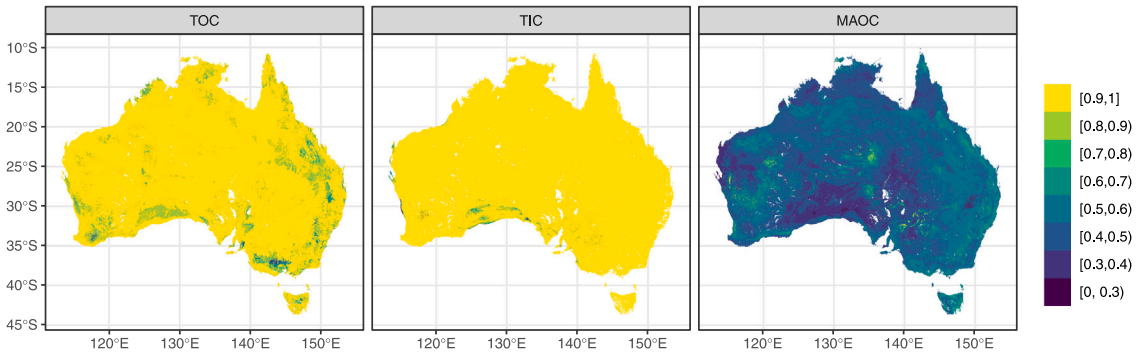

Fig. 8. Maps of the three indicators of condition obtained after averaging by profile.

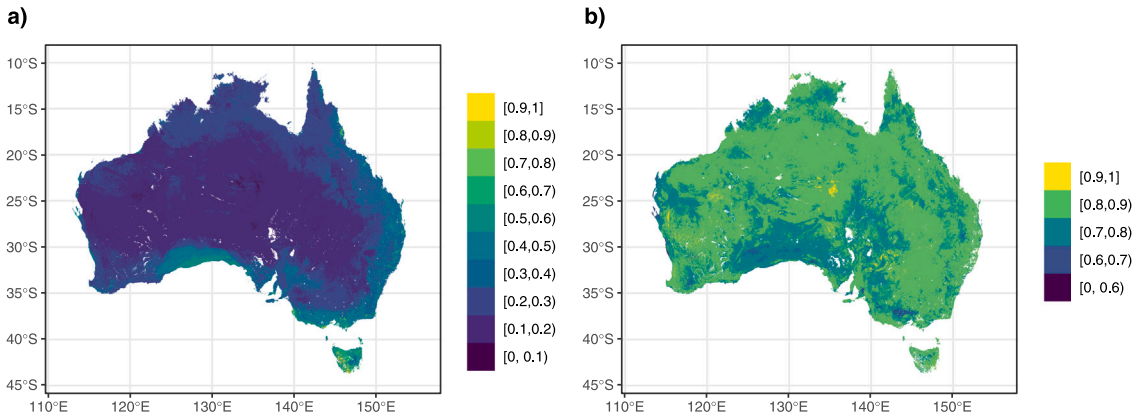

Fig. 9. Maps of (a) capacity and (b) condition of Australia after aggregation by profile and by dimension.

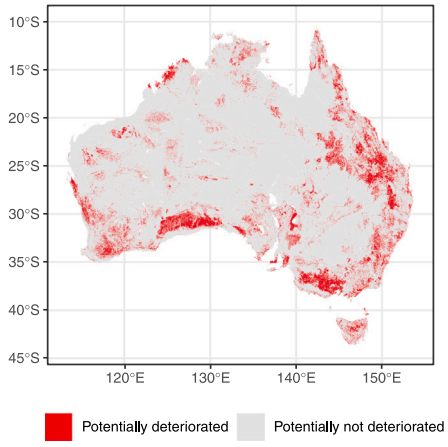

Fig. 10. Map showing areas where the condition is possibly degraded in topsoil TOC (i.e. 0–30 cm) due to agriculture.

grasslands) would allow to include land use in the GAM model and likely further reduce the condition in the cropping areas. For the same reason, it was not possible to apply the genosoil vs phenosoil approach to MAOC storage. However, land use was included indirectly by the parametric terms of the model by assigning different coefficients to regions dominated by pastures or cropping. There were noticeable differences between the average scores of condition produced with the genosoil vs phenosoil assessment (TOC and TIC) and the C saturation model (MAOC). These differences could be caused by the difference in chosen indicator (difference or ratio between current and potential C concentration), as well as the method itself. Applying the genosoil vs phenosoil to MAOC content would have increased consistency in assessment methods, but there we not enough locations with MAOC predictions, and most of these were in agricultural areas, to apply this method. Moreover, the concept of C saturation in the fine fraction reflects well the notion of soil capacity, since the maximum ability to perform the C storage function is estimated with inherent soil properties (silt + clay %). Indeed, empirical models for estimating the upper limit of MAOC storage are well represented in the literature (e.g. Six et al., 2002; Feng et al., 2013; Wiesmeier et al., 2015; Alvarez and Berhongaray, 2021) so we deemed it appropriate for estimating capacity and condition of MAOC storage.

Calculating the soil condition relative to its potential boils down to the definition of capacity (Evangelista et al., 2023a) using the genosoil vs phenosoil assessment. In this assessment, we measure the function fulfilment for a soil relatively unaltered by human forcing and compare it to a similar soil, but with a different land use history. It is essential to capture the relative change between capacity and condition. In this study we only used the difference between the current content and the content of the indicator for capacity for TOC and TIC, and a ratio between the mean and upper limits for the MAOC. In future studies we might explore indices based on ratios or a relative index of change from the genosoil to estimate condition (e.g. $\text{Condition} = u(\text{TOC}_{\text{genosoil}} - \text{TOC}_{\text{phenosoil}} / \text{TOC}_{\text{genosoil}})$). This would not always give high scores for condition when the difference is very small, especially in areas with naturally low TIC and TOC contents. Anther solution to not have high score of condition when the difference is small is to change the shape of the utility graphs from a linear to a smooth function that better accounts for small and gradual changes in the indicator values.

Example functions are the (inverse) of the cumulative distribution function (used, for example in Fine et al., 2017) or with more complex and flexible parameterized functions (e.g. the four-parameter Gompertz curve).

The choice of threshold above which the function is fulfilled was a critical step of our approach. In the literature the threshold is usually given by (local) expertise, obtained from the literature or by using the distribution of the indicator data. In Rabot et al. (2022), for example, most indicators are scored by local expertise for three land uses and the final function fulfilment is taken by proportion of indicators that are above the threshold. A similar approach based on expert knowledge is used in the hierarchical decision support system tool presented in Debeljak et al. (2019) or in the Muencheberg Soil Quality Rating (Mueller et al., 2007). In Alvarez and Berhongaray (2021) and Georgiou et al. (2022) the threshold for MAOC capacity is determined from the 75th and 95th percentile of MAOC, respectively. Alternatively, threshold could also be obtained from physical modelling of the function. This would be the preferred approach but it requires more data and might be computationally demanding. In contrast to approaches based on lookup tables that give an ordinal value of the function, our approach is based on allows for gradual change in the function fulfilment by means of continuous functions (Vogel et al., 2019; Andrews et al., 2004). However, a more thorough analysis is needed to define a reference source of the function fulfilment for different soil types, climatic regions, vegetation, and that meets the demand of users.

The aggregation of different indicators into a single utility measure was obtained by through averaging at two levels: at the profile and by dimension. We considered it a sensible choice since we had no information to suggest that the indicators should have unequal weights. The choice of aggregation method, however, might results in different maps (Greiner et al., 2018). In the future we might consider aggregation using the minimum, the harmonic or geometric mean. Fuzzy and weighted aggregation (McBratney and Odeh, 1997) might circumvent some of the issues linked to the loss of information when aggregating. Aggregation of various indicators into a single dimension provides a summarized information that does not allow one to understand the relative contribution of individual indicators. Using bar charts of pie charts (as in Calzolari et al., 2016, for aggregating of various soil functions) might generate more information for users and decision makers.

In terms of considering a soil *secure*, a soil that has been least affected by human activities should be in good condition relative to its capacity. Hence the choice of genosoils as reference state for assessing condition. However, a *reference* to assess condition is not necessarily the same as the management *target*. When the objective is reaching the maximum performance for a soil function, this (potential) might correspond to a phenosoil that has improved its condition relative to the genosoil (Evangelista et al., 2023b). In multiple studies the targets are estimated empirically as the upper percentiles from the observed distribution of the chosen indicator in a study area.

Beyond the quantification of a single function, there is need to acknowledge the broader picture when framing soil's contributions to sustainable development. The key soil functions are not to be considered separately but part of a broader characterization of the soils recognizing soil services and threats to soils, well addressed by the concept of soil security. The United Nations have specified targets and indicators to reach a sustainable by 2030. Soils contribute to several ecosystem services which in turn relates to land-related sustainable development goals (SDG) such as SDG 2 (food), SDG 6 (water), SDG 13 (climate) and SDG 15 (biodiversity) (Bouma, 2014; Keesstra et al., 2016). Considering the various contributions of soils to ecosystem services require transdisciplinary approaches but also accounting of the opinions and experiences of land-users (Bouma, 2022) through participatory approaches (Wadoux and McBratney, 2023) and gathering of new data and knowledge where missing. The approach proposed in this manuscript is a first step for a systematic evaluation of functions, services and threats, emphasizing the concept of soil security as a roadmap to towards a sustainable development (Bouma, 2020).

5. Conclusion

This study was an initial attempt to implement the soil security assessment framework (Evangelista et al., 2023a) for the function soil as a store of carbon and for the two dimensions of capacity and condition. The methodology consists of three steps, which we applied to the whole of Australia using the three soil indicators and maps of landuse and pedogenons to estimate their reference values. From the results and discussion we draw the following conclusions:

- The model or method used to estimate the indicators has a strong influence on the maps of capacity and condition, as shown by the large differences between the TOC and TIC (genosoil vs phenosoil assessment) and MAOC scores.
- The carbon loss for Australia estimated by global studies did not translate well into lower scores condition for TOC and MAOC, in particular in the wheatbelt of Australia. This may result from undersampling of the genosoils. A targeted sampling effort for soil organic and inorganic carbon in the genosoils is a clear priority. An up-to-date sampling of the phenosoils would also be helpful.
- Estimating the relative change from capacity and condition is hampered by the shape of the utility graph. Using smooth, continuous functions might yield better estimates of the gradual and small changes in the indicator values.
- There might be large uncertainties associated with the input maps, shape of the utility graph and threshold value. Accounting for these various uncertainty sources may be investigated more closely in future research.
- The choice of threshold above which the function is fulfilled, i.e, the utility is unity, is a critical step in our approach, for which there exists no clear reference value. Future research may need to define a reference source of the function fulfilment for different soil types, climatic regions, vegetation, and that meets the demand of users.
- Aggregation of the different indicators into a single dimension using simple averaging almost inevitably resulted in a loss of information. We might explore in the future solutions based on fuzzy or weighted aggregation, or using charts that generate more information for the end users and decision makers.

Beyond fulfilling the objective of a first large-scale evaluation of a soil function following the soil security assessment framework, the capacity and condition maps suggest areas where we need intervention to increase the carbon through management. Most of Australian cropland are already under zero-tillage, but this local index can suggest areas where we lost carbon relative to an unaltered state. In the longer term, we also provide a basis for locating areas that could benefit from carbon crediting schemes.

Declaration of competing interest

All authors have participated in (a) conception and design, or analysis and interpretation of the data; (b) drafting the article or revising it critically for important intellectual content; and (c) approval of the final version.

This manuscript has not been submitted to, nor is under review at, another journal or other publishing venue.

The authors have no affiliation with any organization with a direct or indirect financial interest in the subject matter discussed in the manuscript

Data availability

Data will be made available on request.

Acknowledgements

We acknowledge the support of the Australian Research Council Laureate Fellowship, Australia (FL210100054) on Soil Security entitled "A calculable approach to securing Australia's soil". For the purpose of Open Access, a CC-BY public copyright licence has been applied by the authors to the present document and will be applied to all subsequent versions up to the Author Accepted Manuscript arising from this submission.

References

ABARES, 2021. Catchment Scale Land Use of Australia - Update December 2020. Australian Bureau of Agricultural and Resource Economics and Sciences, Canberra, http://dx.doi.org/10.25814/aqjw-rq15, [dataset] [Accessed: 2023-05-30].

Alvarez, R., Berhongaray, G., 2021. Soil organic carbon sequestration potential of Pampean soils: comparing methods and estimation for surface and deep layers. Soil Res. 59 (4), 346–358.

Andrews, S.S., Karlen, D.L., Cambardella, C.A., 2004. The soil management assessment framework: A quantitative soil quality evaluation method. Soil Sci. Am. J. 68 (6), 1945–1962.

Arshad, M.A., Coen, G.M., 1992. Characterization of soil quality: physical and chemical criteria. Am. J. Altern. Agric. 7 (1–2), 25–31.

Baldock, J.A., Hawke, B., Sanderman, J., Macdonald, L.M., 2013b. Predicting contents of carbon and its component fractions in Australian soils from diffuse reflectance mid-infrared spectra. Soil Res. 51 (8), 577–595.

Baldock, J., Sanderman, J., Macdonald, L., Puccini, A., Hawke, B., Szarvas, S., McGowan, J., 2013a. Quantifying the allocation of soil organic carbon to biologically significant fractions. Soil Res. 51 (8), 561–576.

Baveye, P.C., Baveye, J., Gowdy, J., 2016. Soil "ecosystem" services and natural capital: critical appraisal of research on uncertain ground. Front. Environ. Sci. 4, 41.

Begill, N., Don, A., Poeplau, C., 2023. No detectable upper limit of mineral-associated organic carbon in temperate agricultural soils. Global Change Biol..

Bishop, T.F.A., McBratney, A.B., Laslett, G.M., 1999. Modelling soil attribute depth functions with equal-area quadratic smoothing splines. Geoderma 91 (1–2), 27–45.

Bouma, J., 2014. Soil science contributions towards sustainable development goals and their implementation: linking soil functions with ecosystem services. J. Plant Nutr. Soil Sci. 177 (2), 111–120.

Bouma, J., 2020. Soil security as a roadmap focusing soil contributions on sustainable development agendas. Soil Secur. 1, 100001.

Bouma, J., 2022. How about the role of farmers and of pragmatic approaches when aiming for sustainable development by 2030? Eur. J. Soil Sci. 73 (1), e13166.

Breiman, L., 2001. Random forests. Mach. Learn. 45 (1), 5–32.

Breure, A., De Deyn, G., Dominati, E., Eglin, T., Hedlund, K., Van Orshoven, J., Posthuma, L., 2012. Ecosystem services: a useful concept for soil policy making!. Curr. Opin. Environ. Sustain. 4 (5), 578–585.

Bünemann, E.K., Bongiorno, G., Bai, Z., Creamer, R.E., De Deyn, G., De Goede, R., Fleskens, L., Geissen, V., Kuyper, T.W., Mäder, P., et al., 2018. Soil quality–a critical review. Soil Biol. Biochem. 120, 105–125.

Bureau of Meteorology, 2023. Climate classification maps. http://www.bom.gov.au/climate/maps/averages/climate-classification/?maptype=kpngrp. [Accessed: 2023-05-30].

Calzolari, C., Ungaro, F., Filippi, N., Guermandi, M., Malucelli, F., Marchi, N., Staffilani, F., Tarocco, P., 2016. A methodological framework to assess the multiple contributions of soils to ecosystem services delivery at regional scale. Geoderma 261, 190–203.

de Caritat, P., Bloch, J., Hutcheon, I., 1994. LPNORM: A linear programming normative analysis code. Comput. Geosci. 20 (3), 313–347.

de Caritat, P., Cooper, M., Lech, M., McPherson, A., Thun, C., 2009. National geochemical survey of Australia: Sample preparation manual. Geoscience Australia Record, 2009/08.

Choquet, P., Gabrielle, B., Chalhoub, M., Michelin, J., Sauzet, O., Scammacca, O., Garnier, P., Baveye, P.C., Montagne, D., 2021. Comparison of empirical and process-based modelling to quantify soil-supported ecosystem services on the Saclay plateau (France). Ecosyst. Serv. 50, 101332.

Cotrufo, M.F., Ranalli, M.G., Haddix, M.L., Six, J., Lugato, E., 2019. Soil carbon storage informed by particulate and mineral-associated organic matter. Nat. Geosci. 12 (12), 989–994.

Dalal, R.C., Thornton, C.M., Allen, D.E., Owens, J.S., Kopittke, P.M., 2021. Long-term land use change in Australia from native forest decreases all fractions of soil organic carbon, including resistant organic carbon, for cropping but not sown pasture. Agric. Ecosyst. Environ. 311, 107326.

De Caritat, P., Cooper, M., 2011. National Geochemical Survey of Australia: The Geochemical Atlas of Australia. Geoscience Australia, Canberra.

Debeljak, M., Trajanov, A., Kuzmanovski, V., Schröder, J., Sandén, T., Spiegel, H., Wall, D.P., Van de Broek, M., Rutgers, M., Bampa, F., et al., 2019. A field-scale decision support system for assessment and management of soil functions. Front. Environ. Sci. 7, 115.

Doetterl, S., Stevens, A., Six, J., Merckx, R., Van Oost, K., Casanova Pinto, M., Casanova-Katny, A., Muñoz, C., Boudin, M., Zagal Venegas, E., et al., 2015. Soil carbon storage controlled by interactions between geochemistry and climate. Nat. Geosci. 8 (10), 780–783.

Doran, J.W., Parkin, T.B., 1994. Defining and assessing soil quality. In: Doran, J., Coleman, D., Bezdicek, D., Stewart, B. (Eds.), Defining Soil Quality for a Sustainable Environment. In: SSSA Special Publications, vol. 35, Wiley Online Library, pp. 1–21.

European Commission, 2006a. Proposal for a Directive of the European Parliament and of the Council Establishing a Framework for the Protection of Soil and Amending Directive 2004/35/EC. European Commission Brussels, Belgium.

European Commission, 2006b. Communication from the Commission to the Council, the European Parliament, the European Economic and Social Committee and the Committee of the Regions, Thematic Strategy for Soil Protection. European Commission Brussels, Belgium.

Evangelista, S.J., Field, D.J., McBratney, A.B., Minasny, B., Ng, W., Padarian, J., Román Dobarco, M., Wadoux, A.M.J.-C., 2023a. A proposal for the assessment of soil security: soil functions, soil services and threats to soil. Soil Secur. 10, 100086.

Evangelista, S.J., Field, D.J., McBratney, A.B., Minasny, B., Ng, W., Padarian, J., Román Dobarco, M., Wadoux, A.M.J.-C., 2023b. Soil security - strategising a sustainable future for soil. Adv. Agron. 183.

FAO, ITPS, 2015. Status of the World's Soil Resources – Main Report. Food and Agriculture Organization of the United Nations and Intergovernmental Technical Panel on Soils, Rome, Italy.

Fasiolo, M., Wood, S.N., Zaffran, M., Nedellec, R., Goude, Y., 2021. Qgam: Bayesian nonparametric quantile regression modeling in R. J. Stat. Softw. 100 (9).

Feng, W., Plante, A.F., Six, J., 2013. Improving estimates of maximal organic carbon stabilization by fine soil particles. Biogeochemistry 112, 81–93.

Fine, A.K., van Es, H.M., Schindelbeck, R.R., 2017. Statistics, scoring functions, and regional analysis of a comprehensive soil health database. Soil Sci. Am. J. 81 (3), 589–601.

Georgiou, K., Jackson, R.B., Vindušková, O., Abramoff, R.Z., Ahlström, A., Feng, W., Harden, J.W., Pellegrini, A.F.A., Polley, H.W., Soong, J.L., Riley, W.J., Torn, M.S., 2022. Global stocks and capacity of mineral-associated soil organic carbon. Nature Commun. 13 (1), 3797.

Gray, J.M., Bishop, T.F.A., 2016. Change in soil organic carbon stocks under 12 climate change projections over New South Wales, Australia. Soil Sci. Am. J. 80 (5), 1296–1307.

Gray, J., Karunaratne, S., Bishop, T.F.A., Wilson, B., Veeragathipillai, M., 2019. Driving factors of soil organic carbon fractions over New South Wales, Australia. Geoderma 353, 213–226.

Greiner, L., Keller, A., Grêt-Regamey, A., Papritz, A., 2017. Soil function assessment: review of methods for quantifying the contributions of soils to ecosystem services. Land Use Policy 69, 224–237.

Greiner, L., Nussbaum, M., Papritz, A., Fraefel, M., Zimmermann, S., Schwab, P., Grêt-Regamey, A., Keller, A., 2018. Assessment of soil multi-functionality to support the sustainable use of soil resources on the Swiss Plateau. Geoderma Reg. 14, e00181.

Guo, L.B., Gifford, R.M., 2002. Soil carbon stocks and land use change: a meta analysis. Global Change Biol. 8 (4), 345–360.

Hicks, W., Viscarra Rossel, R.A., Tuomi, S., 2015. Developing the Australian mid-infrared spectroscopic database using data from the Australian soil resource information system. Soil Res. 53 (8), 922–931.

Isbell, R., National Committee on Soil and Terrain, 2021. The Australian Soil Classification, third ed. CSIRO publishing, Canberra.

Keesstra, S.D., Bouma, J., Wallinga, J., Tittonell, P., Smith, P., Cerdà, A., Montanarella, L., Quinton, J., Pachepsky, Y., Van Der Putten, W.H., et al., 2016. The significance of soils and soil science towards realization of the UN sustainable development goals (SDGS). SOIL 2016, 1–28.

Lech, M.E., de Caritat, P., McPherson, A.A., 2007. National geochemical survey of australia: field manual. Geoscience Australia Record, 2007/08, 53.

Lehmann, J., Bossio, D.A., Kögel-Knabner, I., Rillig, M.C., 2020. The concept and future prospects of soil health. Nat. Rev. Earth Environ. 1 (10), 544–553.

Malone, B., 2020. Soil Carbon Fraction Modelling Via Vis-NIR Spectroscopy. CSIRO, Australia.

Malone, B.P., McBratney, A.B., Minasny, B., Laslett, G.M., 2009. Mapping continuous depth functions of soil carbon storage and available water capacity. Geoderma 154 (1–2), 138–152.

Malone, B., Searle, R., 2021. Updating the Australian digital soil texture mapping (part 2): spatial modelling of merged field and lab measurements. Soil Res. 59 (5), 435–451.

Malone, B., Stockmann, U., Tuomi, S., Sparrow, B., 2020. Soil and landscape grid national soil attribute maps - organic carbon (1" resolution). http://dx.doi.org/10.25919/9bya-9545, TERN Surveillance monitoring program: Soil vis-NIR spectral library with accompanying soil measurement data for 367 specimens v1. [dataset].

Malone, B., Wadoux, A.M.J.-C., 2022. Soil Carbon Fraction Model Development and Extension: A Case of Instrument Transfer and Assessment of Model Extensibility. CSIRO, Australia.

McBratney, A., Field, D.J., Koch, A., 2014. The dimensions of soil security. Geoderma 213, 203–213.

McBratney, A.B., Odeh, I.O., 1997. Application of fuzzy sets in soil science: fuzzy logic, fuzzy measurements and fuzzy decisions. Geoderma 77 (2–4), 85–113.

Mueller, L., Schindler, U., Behrendt, A., Eulenstein, F., Dannowski, R., 2007. The Muencheberg Soil Quality Rating. SQR, Leibniz-Centre for Agricultural Landscape Research (ZALF) e. V., Muencheberg, Germany.

Nortcliff, S., 2002. Standardisation of soil quality attributes. Agric. Ecosyst. Environ. 88 (2), 161–168.

Rabot, E., Guiresse, M., Pittatore, Y., Angelini, M., Keller, C., Lagacherie, P., 2022. Development and spatialization of a soil potential multifunctionality index for agriculture (agri-SPMI) at the regional scale. Case study in the occitanie region (France). Soil Secur. 6, 100034.

Rinot, O., Levy, G.J., Steinberger, Y., Svoray, T., Eshel, G., 2019. Soil health assessment: A critical review of current methodologies and a proposed new approach. Sci. Total Environ. 648, 1484–1491.

Rocci, K.S., Lavallee, J.M., Stewart, C.E., Cotrufo, M.F., 2021. Soil organic carbon response to global environmental change depends on its distribution between mineral-associated and particulate organic matter: A meta-analysis. Sci. Total Environ. 793, 148569.

Román Dobarco, M., McBratney, A., Minasny, B., Malone, B., 2021a. A framework to assess changes in soil condition and capability over large areas. Soil Secur. 4, 100011.

Román Dobarco, M., McBratney, A.B., Minasny, B., Malone, B., 2021b. A modelling framework for pedogenon mapping. Geoderma 393, 115012.

Román Dobarco, M., McBratney, A.B., Minasny, B., Malone, B., 2022. Soil and landscape grid national soil attribute maps - pedogenons (3" resolution). http://dx.doi.org/10.25919/r8rv-8617, Release 1. v1. Commonwealth Scientific and Industrial Research Organisation (CSIRO).

Román Dobarco, M., Padarian Campusano, J., McBratney, A.B., Malone, B., Minasny, B., 2023a. Genosoil and phenosoil mapping in continental Australia is essential for soil security. Soil Secur. 100108.

Román Dobarco, M., Wadoux, A.M.J.-C., Malone, B., Minasny, B., McBratney, A.B., Searle, R., 2023b. Mapping soil organic carbon fractions for Australia, their stocks and uncertainty. Biogeosciences 20, 1–38.

Rossiter, D.G., 1996. A theoretical framework for land evaluation. Geoderma 72 (3–4), 165–190.

Rossiter, D.G., Bouma, J., 2018. A new look at soil phenoforms–definition, identification, mapping. Geoderma 314, 113–121.

Sanderman, J., Hengl, T., Fiske, G.J., 2017. Soil carbon debt of 12,000 years of human land use. Proc. Natl. Acad. Sci. 114 (36), 9575–9580.

Searle, R., Malone, B., Wilford, J., Austin, J., Ware, C., Webb, M., Romàn Dobarco, M., Van Niel, T., 2022. Soil carbon fraction modelling via vis-NIR spectroscopy. http://dx.doi.org/10.25919/jr32-yq58, TERN Digital Soil Mapping Raster Covariate Stacks. v2. CSIRO. Data Collection.

Searle, R., Stenson, M., Wilson, P.L., Gregory, L.J., Singh, R., Malone, B.P., 2021. Soil Data, United, Will Never Be Defeated – the Soildatafederator. Joint Australian and New Zealand Soil Science Societies Conference, Cairns, QLD.

Seybold, C.A., Mansbach, M.J., Karlen, D.L., Rogers, H.H., 2018. Quantification of soil quality. In: Soil Processes and the Carbon Cycle. CRC Press, pp. 387–404.

Sharififar, A., Minasny, B., Arrouays, D., Boulonne, L., Chevallier, T., van Deventer, P., Field, D.J., Gomez, C., Jang, H.-J., Jeon, S.-H., Koch, J., McBratney, A.B., Malone, B.P., Marchant, B.P., Martin, M.P., Monger, C., Munera-Echeverri, J.-L., Padarian, J., Pfeiffer, M., de Forges, A.C.R., Saby, N.P., Singh, K., Song, X.-D., Zamanian, K., Zhang, G.-L., van Zijl, G., 2023. Soil inorganic carbon, the other and equally important soil carbon pool: distribution, controlling factors, and the impact of climate change. In: Sparks, D.L. (Ed.), Advances in Agronomy. Vol. 178, Elsevier.

Six, J., Conant, R., Paul, E., Paustian, K., 2002. Stabilization mechanisms of soil organic matter: Implications for C-saturation of soils. Plant Soil 241 (2), 155–176.

Stewart, C.E., Paustian, K., Conant, R.T., Plante, A.F., Six, J., 2007. Soil carbon saturation: concept, evidence and evaluation. Biogeochemistry 86, 19–31.

Styc, Q., Lagacherie, P., 2019. What is the best inference trajectory for mapping soil functions: An example of mapping soil available water capacity over Languedoc Roussillon (France). Soil Syst. 3 (2), 34.

Van Leeuwen, J.P., Creamer, R.E., Cluzeau, D., Debeljak, M., Gatti, F., Henriksen, C.B., Kuzmanovski, V., Menta, C., Pérès, G., Picaud, C., et al., 2019. Modeling of soil functions for assessing soil quality: Soil biodiversity and habitat provisioning. Front. Environ. Sci. 7, 113.

Viscarra Rossel, R.A., Hicks, W.S., 2015. Soil organic carbon and its fractions estimated by visible–near infrared transfer functions. Eur. J. Soil Sci. 66 (3), 438–450.

Vogel, H.-J., Bartke, S., Daedlow, K., Helming, K., Kögel-Knabner, I., Lang, B., Rabot, E., Russell, D., Stößel, B., Weller, U., et al., 2018. A systemic approach for modeling soil functions. SOIL 4 (1), 83–92.

Vogel, H.-J., Eberhardt, E., Franko, U., Lang, B., Ließ, M., Weller, U., Wiesmeier, M., Wollschläger, U., 2019. Quantitative evaluation of soil functions: Potential and state. Front. Environ. Sci. 7, 164.

von Lützow, M., Kögel-Knabner, I., Ekschmitt, K., Matzner, E., Guggenberger, G., Marschner, B., Flessa, H., 2006. Stabilization of organic matter in temperate soils: mechanisms and their relevance under different soil conditions–a review. Eur. J. Soil Sci. 57 (4), 426–445.

Vrebos, D., Jones, A., Lugato, E., O'Sullivan, L., Schulte, R., Staes, J., Meire, P., 2021. Spatial evaluation and trade-off analysis of soil functions through Bayesian networks. Eur. J. Soil Sci. 72 (4), 1575–1589.

Wadoux, A.M.J.-C., Heuvelink, G.B.M., Lark, R.M., Lagacherie, P., Bouma, J., Mulder, V.L., Libohova, Z., Yang, L., McBratney, A.B., 2021. Ten challenges for the future of pedometrics. Geoderma 401, 115155.

Wadoux, A.M.J.-C., McBratney, A.B., 2023. Participatory approaches for soil research and management: A literature-based synthesis. Soil Secur. 100085.

Wadoux, A.M.J.-C., Román Dobarco, M., Malone, B., Minasny, B., McBratney, A.B., Searle, R., 2022. Soil and landscape grid national soil attribute maps - organic carbon (1" resolution). http://dx.doi.org/10.25919/07c3-2n73, Release 1. v1. Commonwealth Scientific and Industrial Research Organisation (CSIRO), Canberra, Australia.

Wadoux, A.M.J.-C., Román Dobarco, M., Malone, B., Minasny, B., McBratney, A.B., Searle, R., 2023. Baseline high-resolution maps of organic carbon content in Australian soils. Sci. Data 10, 181.

Wang, B., Waters, C., Orgill, S., Gray, J., Cowie, A., Clark, A., Li Liu, D., 2018. High resolution mapping of soil organic carbon stocks using remote sensing variables in the semi-arid rangelands of eastern Australia. Sci. Total Environ. 630, 367–378.

Wells, T., Hancock, G.R., Martinez, C., Dever, C., Kunkel, V., Gibson, A., 2019. Differences in soil organic carbon and soil erosion for native pasture and minimum till agricultural management systems. Sci. Total Environ. 666, 618–630.

Wiesmeier, M., Munro, S., Barthold, F., Steffens, M., Schad, P., Kögel-Knabner, I., 2015. Carbon storage capacity of semi-arid grassland soils and sequestration potentials in northern China. Global Change Biol. 21 (10), 3836–3845.

Wood, S., 2022. Mgcv: Mixed GAM computation vehicle with automatic smoothness estimation. URL: https://CRAN.R-project.org/package=mgcv. R package version 1.8-40. Accessed 23.09.2022.

Zwetsloot, M.J., van Leeuwen, J., Hemerik, L., Martens, H., Simo Josa, I., Van de Broek, M., Debeljak, M., Rutgers, M., Sandén, T., Wall, D.P., et al., 2021. Soil multifunctionality: Synergies and trade-offs across European climatic zones and land uses. Eur. J. Soil Sci. 72 (4), 1640–1654.